DOI: 10.1002/cmdc.201100098

Novel Mechanism of Cathepsin B Inhibition by Antibiotic Nitroxoline and Related Compounds

Bojana Mirković,[a] Miha Renko,[b] Samo Turk,[a] Izidor Sosič,[a] Zala Jevnikar,[a] Nataša Obermajer,[a, c] Dušan Turk,[b] Stanislav Gobec,[a] and Janko Kos*[a, c]

Cathepsin B (EC 3.4.22.1) represents a promising therapeutic target in various diseases associated with its aberrant activity. The most noted is its role in the degradation of extracellular matrix (ECM) proteins in tumor tissues, enabling tumor cells to migrate, invade adjacent barriers, and metastasize.[1,2] It is unique among cathepsins in possessing both endopeptidase and dipeptidyl carboxypeptidase activities.[3] This dual character is attributed to the presence of a 21-amino-acid insertion termed the occluding loop.[4] In the exopeptidase conformation, the loop is attached to the enzyme body, limiting the binding of extended substrates to the primed sites of the active site cleft.[5] However, the loop is flexible, and the endopeptidase activity is increased dramatically on removal of the contacts that bind it to the enzyme,[6] resulting in its harmful action in pathological processes.

Cathepsin B activity is regulated by endogenous protein inhibitors, the cystatins.[1] However, these are general cysteine protease inhibitors, and as such are not appropriate for therapeutic applications. Many classes of synthetic cathepsin B inhibitors have been described.[7] The majority of these contain peptidyl backbones with an electrophilic reactive group that forms a covalent bond with an amino acid residue in the active site of the enzyme. None of the known cathepsin B inhibitors are in clinical use due to poor bioavailability, off-target side effects, and high toxicity.[8] Therefore, considering the high pharmacological relevance of cathepsin B, the identification of new small-molecule inhibitors capable of binding reversibly and selectively to the enzyme, with improved oral bioavailability, needs to be given greater emphasis.

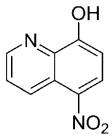

Nitroxoline (**1**)

In this study, using virtual high-throughput screening followed by biological evaluation of the best ranked compounds against different cathepsins, we discovered that nitroxoline (5-nitro-8-hydroxyquinoline; **1**), a well-established antimicrobial agent used for the treatment of urinary tract infections,[9] is a potent and reversible inhibitor of cathepsin B. However, in the case of nitroxoline, interactions with proteolytic enzymes have not been reported to impair its basic antimicrobial function. The toxicity of nitroxoline is low, and no serious adverse effects have been reported in association with nitroxoline therapy in humans (http://ccinfoweb.ccohs.ca/rtecs/search.html). From this point of view, cathepsin B as a new off-target for nitroxoline provides potential applications in additional therapeutic categories rather than insights into molecular mechanisms of drug side effects.

The K_i value for the interaction of nitroxoline with cathepsin B and the mode by which it impairs its activity were determined by enzyme kinetics. First, the effect of nitroxoline on cathepsin B activity was assessed using the Z-Arg-Arg-AMC substrate, which is commonly used to determine the endopeptidase activity of cathepsin B,[10–12] although it is only able to interact with the S1′ subsite of cathepsin B.[6] Using this substrate, nitroxoline was determined to be a mixed inhibitor of cathepsin B. The K_i' value for dissociation of the ezyme–substrate–inhibitor (ESI) complex is in the low micromolar range (39.5 ± 2.8 μM; Table 1) and is 3.9-fold lower than the K_i value for dissociation of the EI complex. This indicates that nitroxoline binds to the ES complex with greater affinity than to the free enzyme. Furthermore, cathepsin B inhibition by nitroxoline was not impaired by Triton X-100 at 0.005 and 0.01%, excluding the possibility of promiscuous inhibition[13] (see figure S1 in the Supporting Information) and confirming nitroxoline as a true inhibitor of cathepsin B.

Table 1. K_i values for the inhibition of cathepsins B, H and L by nitroxoline (**1**).[a]

Cathepsin	Substrate	K_i [μM]	K_i' [μM]
B	Z-Arg-Arg-AMC	154.4 ± 26.7[b]	39.5 ± 2.8[b]
B	Abz-Gly-Ile-Val-Arg-Ala-Lys(Dnp)-OH	271.8 ± 22.8[c]	–
H	Arg-AMC	290.5 ± 25.0[c]	–
L	Z-Phe-Arg-AMC	191.3 ± 12.3[c]	–

[a] Data represent the mean ± SD ($n = 2$). [b] Mixed inhibition with a predominantly uncompetitive component. [c] Noncompetitive inhibition.

The ability of nitroxoline to inhibit cathepsin B dipeptidyl carboxypeptidase activity was determined using the cathepsin B-specific exopeptidase substrate Abz-Gly-Ile-Val-Arg-Ala-Lys(Dnp)-OH. Nitroxoline acted as a noncompetitive inhibitor of the exopeptidase activity, with a K_i value of 271.8 ± 11.2 μM (Table 1), indicating that the inhibitor binds to the free enzyme and the substrate-bound enzyme with the same affinity. K_i and

[a] Dr. B. Mirković, Dr. S. Turk, I. Sosič, Dr. Z. Jevnikar, Dr. N. Obermajer, Prof. Dr. S. Gobec, Prof. Dr. J. Kos
Faculty of Pharmacy, University of Ljubljana
Aškerčeva 7, 1000 Ljubljana (Slovenia)
Fax: (+386) 1-42-58-031
E-mail: janko.kos@ffa.uni-lj.si

[b] Dr. M. Renko, Prof. Dr. D. Turk
Department of Biochemistry, Molecular and Structural Biology
Jožef Stefan Institute
Jamova 39, 1000 Ljubljana (Slovenia)

[c] Dr. N. Obermajer, Prof. Dr. J. Kos
Department of Biotechnology, Jožef Stefan Institute
Jamova 39, 1000 Ljubljana (Slovenia)

Supporting Information for this article is available on the WWW under http://dx.doi.org/10.1002/cmdc.201100098.

K_i' values determined with Abz-Gly-Ile-Val-Arg-Ala-Lys(Dnp)-OH were 1.8-fold and 6.9-fold, respectively, greater than those determined with Z-Arg-Arg-AMC, which indicates a preference of nitroxoline for inhibiting cathepsin B endopeptidase activity.

The mode of inhibition by nitroxoline was shown to be reversible by three independent experiments. In the first, rapid 100-fold dilution of a 5 min incubation mixture of nitroxoline at 10-times the IC_{50} value and cathepsin B at 100-fold final concentration resulted in 78.3 ± 2.2% recovery of the enzyme activity. This is in line with the calculated value (85%), taking into account the Hill coefficient of nitroxoline ($h = 1.69$, $R = 0.9982$), and confirms the reversible inhibition of cathepsin B. Furthermore, the value did not change significantly after 15 and 30 min pre-incubation (74.8 ± 3.5% and 72.4 ± 3.2%, respectively; Figure 1a). In the second experiment, we used an active site probe DCG-04 to test for the reversibility of the inhibitor binding. The intensity of cathepsin B bands treated with nitroxoline did not differ significantly from those of the control (DMSO) over the entire concentration range. On the other hand, the cathepsin B-specific, irreversible inhibitor CA-074 showed concentration-dependant inactivation of cathepsin B, with the band visible only at the lowest concentration of inhibitor (Figure 1b). Finally, the reversibility of nitroxoline was confirmed by mass spectrometry; incubation of cathepsin B with nitroxoline led to no significant change in protein mass. However, when CA-074 was used, the mass of the enzyme increased by 384 Da, as expected for covalent binding of the inhibitor (calculated mass of bound fragment: 384.21 Da; Figure 1c).

Nitroxoline was shown to inhibit aminopeptidase cathepsin H (EC 3.4.22.16) and endopeptidase cathepsin L (EC 3.4.22.15), but more weakly than it does cathepsin B (Table 1). It is a noncompetitive inhibitor of both, with 7.4-fold and 4.8-fold greater K_i' values than that determined for cathepsin B with Z-Arg-Arg-AMC as the substrate.

Next, nitroxoline-related compounds were tested for their inhibition of cathepsin B. 7-Aminomethylated nitroxoline derivatives **2**–**8** exhibited relative inhibition at least as potent as nitroxoline. K_i values for the latter were determined using the substrates Z-Arg-Arg-AMC and Abz-Gly-Ile-Val-Arg-Ala-Lys-(Dnp)-OH. Of the 7-substituted nitroxolines, only compounds **4** and **7** exhibited the same inhibition mode as nitroxoline, that is, mixed inhibition with a predominantly uncompetitive component using Z-Arg-Arg-AMC as the substrate (Table 2). Conversely, compounds **2**, **3**, **5**, **6** and **8** were all noncompetitive inhibitors of cathepsin B activity against Z-Arg-Arg-AMC and,

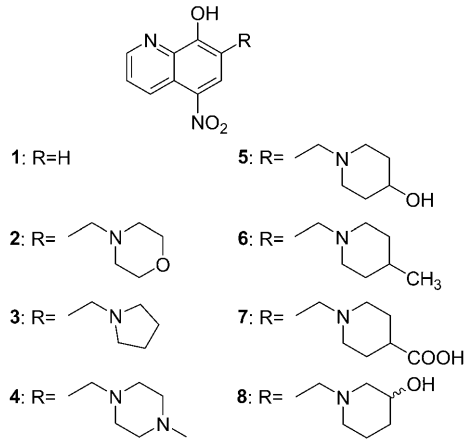

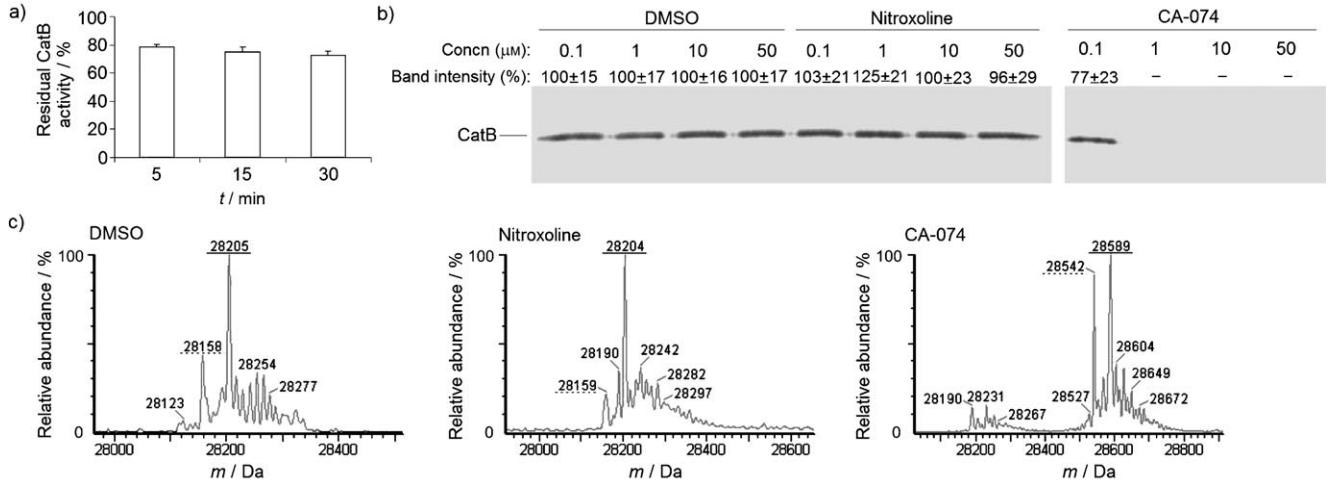

Figure 1. Nitroxoline is a reversible inhibitor of cathepsin B. a) Cathepsin B at a 100-fold final concentration was incubated with nitroxoline at a concentration of 10-times the IC_{50} value. After 5, 15 and 30 min incubation time, the mixture was diluted with substrate, reducing the enzyme concentration to that of a standard assay, and the inhibitor concentration to 0.1-times the IC_{50} value. The recovery of enzyme activity was near the calculated value (85%) for reversible inhibition and did not change significantly with prolonged incubation. Data are presented as a percentage of the DMSO control experiment (mean ± SD, $n = 2$). b) Cathepsin B was incubated with increasing concentrations of nitroxoline and CA-074 and subsequently labeled with DCG-04 (2 μM). Samples were then analyzed with SDS-PAGE and Western blotting. Band intensity correlates with cathepsin B activity. The relative band intensity was obtained by dividing the individual intensity with that of the DMSO control. Data are presented as the mean ± SD. c) Mass spectrometry shows nitroxoline to be a reversible inhibitor of cathepsin B since it did not change the mass of the cathepsin B peak (underlined). Incubation with CA-074 led to a 384 Da increase in mass, as expected.

Table 2. K_i values for nitroxoline (**1**) and its derivatives (**2**–**8**) against cathepsin B using substrates Z-Arg-Arg-AMC and Abz-Gly-Ile-Val-Arg-Ala-Lys-(Dnp)-OH.

Compd	K_i[a] [μM]	K_i'[a] [μM]	K_i[b] [μM]
1	154.4 ± 26.7[c]	39.5 ± 2.8[c]	271.8 ± 11.2[d]
2	118.8 ± 4.2[d]	–	199.7 ± 11.2[d]
3	117.8 ± 3.1[d]	–	108.2 ± 13.4[e]
4	118.5 ± 11.7[c]	52.5 ± 0.8[c]	195.3 ± 14.1[d]
5	129.7 ± 3.4[d]	–	173.2 ± 10.6[d]
6	129.8 ± 3.5[d]	–	116.2 ± 15.4[e]
7	92.9 ± 1.9[c]	66.5 ± 0.4[c]	347.8 ± 16.1[d]
8	109.8 ± 3.1[d]	–	156.1 ± 8.7[d]

[a] K_i and K_i' values were determined with Z-Arg-Arg-AMC. [b] K_i values were determined with Abz-Gly-Ile-Val-Arg-Ala-Lys(Dnp)-OH. [c] Mixed inhibition with a predominantly uncompetitive component. [d] Noncompetitive inhibition. [e] Competitive inhibition. Data represent the mean ± SEM ($n = 2$).

unlike nitroxoline, had the same affinity for both the free and substrate-bound enzyme. Using Z-Arg-Arg-AMC, all compounds **2**–**8** displayed lower affinities for the ES complex than nitroxoline, as evident from the K_i' values, but at the same time possessed higher affinities for the free enzyme, as evident from K_i values. When Abz-Gly-Ile-Val-Arg-Ala-Lys(Dnp)-OH was used as a substrate, compounds **2**, **4**, **5**, **7** and **8** all retained the nitroxoline mode of inhibition, that is, noncompetitive inhibition of cathepsin B exopeptidase activity. With the exception of compound **7**, they were all more potent inhibitors of cathepsin B exopeptidase activity than nitroxoline (271.8 ± 11.2 μM). However, two nitroxoline derivatives, compounds **3** and **6**, competitively inhibited cathepsin B exopeptidase activity while displaying the highest inhibition of cathepsin B exopeptidase activity (Table 2).

In order to reveal the structural requirements of nitroxoline for cathepsin B inhibitory activity, a number of related quinolines (**9**–**25**) were evaluated. The minimum structural motif for cathepsin B inhibition was identified as the 5-nitro-8-hydroxyquinoline core. Removal of either the 5-nitro or 8-hydroxy group leads to almost complete loss of inhibition (table S1 in the Supporting Information). The only exceptions to this generalization were compounds **13** and **21**, which both possess an amino group in position 5 of the quinoline ring system; however, their inhibitory activity was only moderate.

Our results provide the first X-ray crystal structure for the complex of cathepsin B with a reversible, nonpeptidyl inhibitor. Cathepsin B, in complex with nitroxoline, crystallized in a C2 space group, with two molecules in the asymmetric unit. The crystals contained the complete sequence of the active form (numbered Leu 1–Asp 254), with two additional residues at the N terminus (Leu 1 and Lys 0) that remained as a result of autoactivation. Positioning of nearly all the residues is clearly revealed by the electron density maps, with the exception of a few long side chains. The structures of the two cathepsin B molecules in the asymmetric unit are closely related, with a root mean square distance (RMSD) value of 0.44 Å. The crystal structure is also closely related to previously published structures 1CSB[14] and 1GMY,[15] with an RMSD value of equipositioned CA atom (α atom in the amino acid) smaller than 0.5 Å.

The binding of nitroxoline is visible in both molecules in the asymmetric unit. The averaged kick omit $F_o - F_c$ electron density map clearly indicates the position of the molecule (Figure 2a).[16] However, refinement suggests a reduced occupancy of 0.5, which is most probably a consequence of the low concentration of nitroxoline limited by poor solubility. The molar ratio between cathepsin B and nitroxoline reached during the crystallization setup was 1:1.

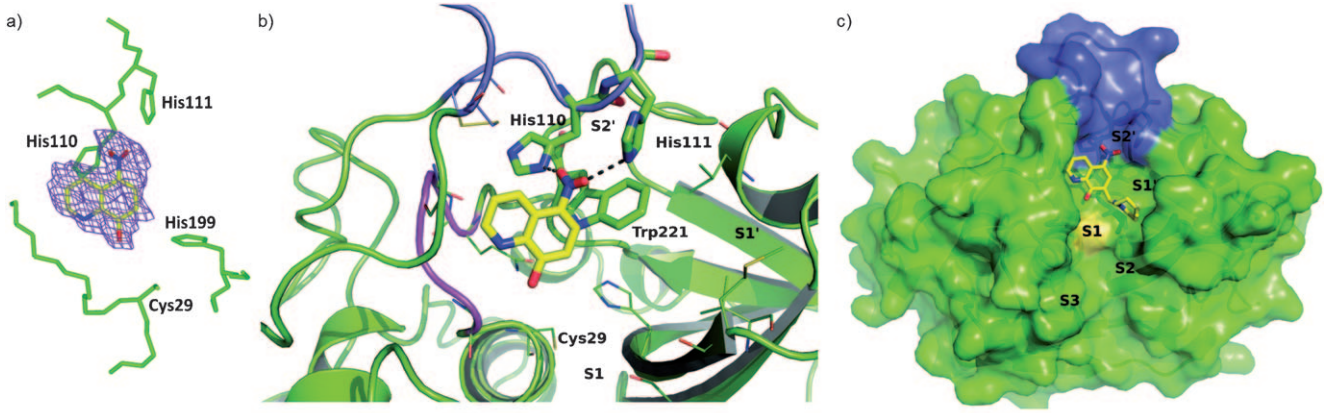

Figure 2. The crystal structure of nitroxoline–cathepsin B complex (PDB: 3AI8). a) The electron density $F_0 - F_c$ (contoured at 1σ) indicates the position of the nitroxoline. The residues Cys 29 and Cys 199 forming the catalytic dyad and two histidines from the occluding loop are shown as green sticks. b) Nitroxoline (yellow) binds to the primed site (S2′) of the cathepsin B active site cleft. The binding surface for the inhibitor is comprised of the loop Gln 23–Gly 27 (pink loop), occluding loop (blue) residues His 110 and His 111, and Trp 221 (green sticks). The negatively charged nitro group is inserted symmetrically between His 110 and His 111, and each oxygen atom interacts with one histidine residue (**-----**). The nitro group lies almost perpendicular to the quinoline rings. Other amino acid residues from S1, S1′ and S2′ are shown as green lines, also catalytic Cys 29 is shown for orientation. c) The model of the binding of compound **6** (yellow) to cathepsin B explains the stronger inhibition of cathepsin B by 7-substituted nitroxolines. Additional rings attached in the 7-position bind in the S1′ binding site, contributing to enhanced inhibition. The active site cysteine is shown as yellow sticks and surface. The occluding loop, His 110 and His 111, are shown in blue.

Nitroxoline binds to the primed site of the active site cleft (Figure 2b). The aromatic quinoline rings fill the S2′ binding site. The binding surface for nitroxoline is provided by the loop Gln23–Gly27, the occluding loop residues His110 and His111, and Trp221. The negatively charged nitro group interacts with His110 and His111, similarly to the carboxylate of the epoxysuccinyl-based irreversible inhibitors CA-030[14] and NS134.[15] In these structures, the carboxylic group of the terminal proline residue binds between the two histidines with one oxygen atom, while the other oxygen atom binds asymmetrically to His111 only. The nitro group of nitroxoline, on the other hand, lies more symmetrically between the two histidines and each oxygen atom interacts with one histidine. The nitro group lies almost perpendicular to the quinoline rings, and this positioning is accompanied by increased separation of the two histidines. The nitrogen atoms ND1 and NE2 of His110 and His111 are 5.9 Å apart in the nitroxoline complex, whereas in the CA-030 and NS134 complexes their separation is 5.3 Å. Thus, the nitro group is seen to be essential for binding nitroxoline to the occluding loop histidines. This is consistent with the inhibition data (table S1 in the Supporting Information), where compounds without the nitro group (**10**–**12**, **14**–**20**, **22**–**25**) showed significantly lower inhibition.

Although the hydroxy group in nitroxoline does not interact with cathepsin B, it is interesting that its removal in compound **9** resulted in significantly lower inhibition. It is possible that lack of the hydrophilic hydroxy group resulted in lower solubility of the compound. The modifications to all other carbon atoms except C7 resulted in significantly lower inhibition. From the crystal structure, it is evident that C7 is the only position that can be functionalized without causing steric clashes. The rings attached at position 7 (compounds **2**–**8**) likely bind into the S1′ binding site and in this way contribute to enhanced inhibition (Figure 2c). This is evident from enzyme kinetic data obtained with Abz-Gly-Ile-Val-Arg-Ala-Lys(Dnp)-OH, where 7-substituted nitroxolines, with the exception of compound **7**, displayed greater inhibition of cathepsin B exopeptidase activity than nitroxoline. The most potent inhibition of exopeptidase activity was achieved with compounds **3** and **6**, which were also the only ones to display competitive inhibition. This is not unexpected since the S1′ subsite favors hydrophobic interactions[17] and the substituents of compounds **3** and **6** are among the most hydrophobic contained in the synthesized nitroxoline derivatives. However, when Z-Arg-Arg-AMC was used, the improvement in inhibition of cathepsin B activity was not as pronounced, which could be a result of substrate subsite

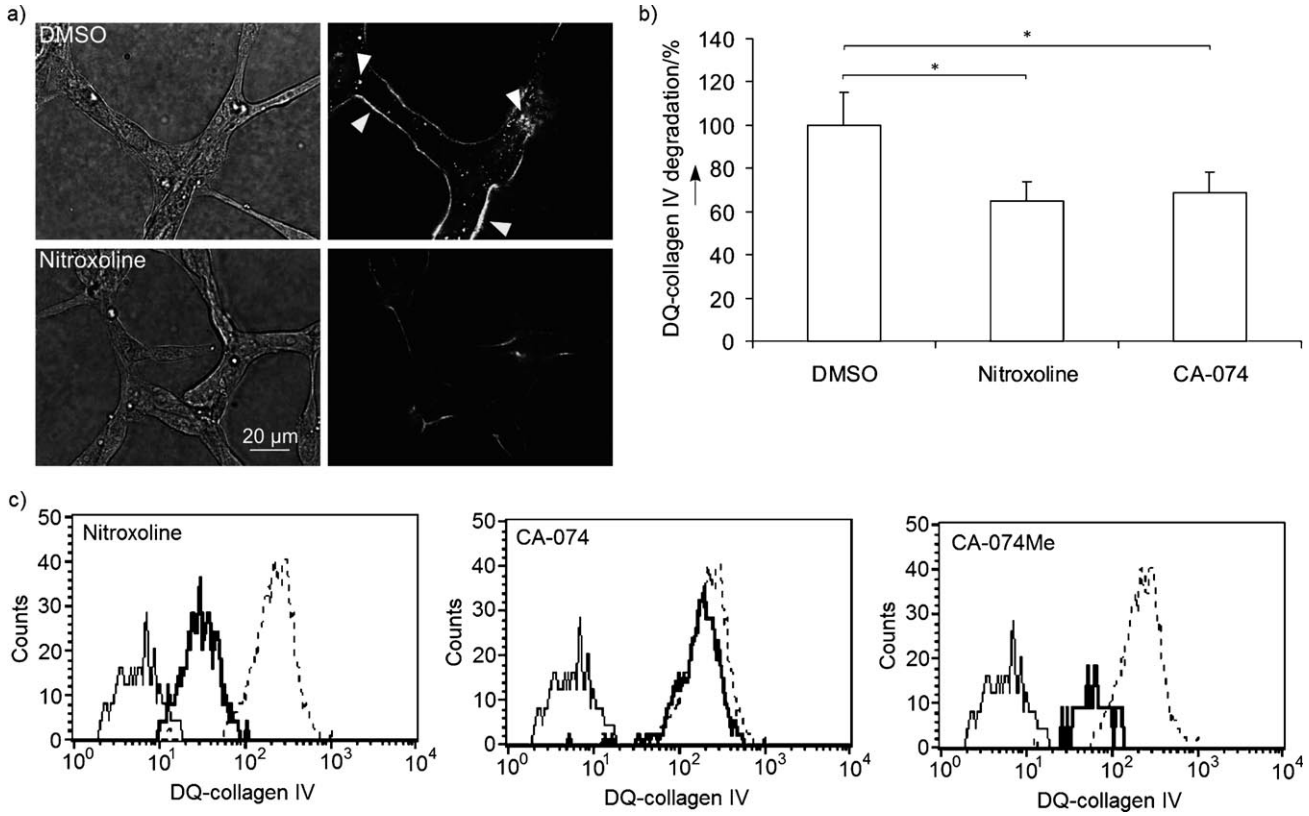

Figure 3. Nitroxoline inhibits DQ–collagen IV degradation by MCF-10A neoT cells. a) MCF-10A neoT cells degrade DQ–collagen IV intracellularly (white arrow) and extracellularly (grey arrow) as shown by fluorescence microscopy. Addition of 10 μM nitroxoline impairs intracellular and extracellular DQ–collagen IV degradation. Left panels are differential interface contrast (DIC) images; right panels are images of green fluorescence following hydrolysis of DQ–collagen IV. b) Inhibition of extracellular DQ–collagen IV degradation by 10 μM nitroxoline (35.3%) and 10 μM CA-074 (31.1%). Data are presented as percentages of DQ–collagen IV degradation compared to the DMSO control (mean ± SD, $n = 6$). The asterisk indicates significant differences ($p < 0.05$) relative to the DMSO control as determined by a two-tailed *t*-test. c) Inhibition of intracellular DQ–collagen IV degradation by nitroxoline (50 μM) as measured by flow cytometry. Inhibition of DQ–collagen IV degradation can be seen as a shift in fluorescence intensity (——) as compared to the control: MCF-10A neoT cells grown in the presence of DMSO (-----). Control cells were grown in the absence of DQ–collagen IV (——). Permeable cathepsin B inhibitor CA-074Me (50 μM) was used as a positive control and also inhibited intracellular degradation of DQ–collagen IV, whereas impermeable cathepsin B inhibitor CA-074 (50 μM) did not.

occupancy. For example, Z-Arg-Arg-AMC covers the sites from S3 to S1′, whereas Abz-Gly-Ile-Val-Arg-Ala-Lys(Dnp)-OH covers the enzyme sites up to the subsite S2′, increasing the chances of steric hindrance between the substrate and inhibitor.

Nitroxoline was also shown to impair cathepsin B activity in cell models mimicking the pathological processes in which cathepsin B is implicated. The proteolytic degradation of ECM by transformed cells was followed by observing fluorescent degradation products of DQ–collagen IV, a major constituent of the extracellular matrix, heavily labeled with fluorescein. Nitroxoline markedly decreased intracellular and extracellular degradation of DQ–collagen IV of MCF-10A neoT cells as shown by fluorescence microscopy (Figure 3a). Extracellular degradation of DQ–collagen IV was quantified in a separate experiment based on the measurement of fluorescent degradation products in the medium of MCF-10A neoT cells. The extracellular degradation of DQ–collagen IV by nitroxoline was inhibited by 35.3%, which is comparable to the inhibition by CA-074 (31.1%), an extracellular cathepsin B inhibitor (Figure 3b). Inhibition of intracellular degradation of DQ–collagen IV by nitroxoline was determined by flow cytometry (Figure 3c). The shift in fluorescence intensity, as a measure of inhibition, was comparable to the shift of the cell permeable cathepsin B inhibitor CA-074Me. In contrast, the impermeable inhibitor of cathepsin B, CA-074, had no effect on intracellular degradation of DQ–collagen IV. The ability of nitroxoline to inhibit both extracellular and intracellular DQ–collagen IV degradation suggests that nitroxoline possesses favorable cell permeability characteristics and is therefore able to enter cells, where it inhibits cathepsin B in endosomal/lysosomal vesicles in addition to membrane-bound and secreted cathepsin B. This is an advantage over the majority of known cathepsin B inhibitors, which exhibit poor cell uptake and bioavailability due to their peptidyl structure.[8] For example, the epoxysuccinyl inhibitor CA-074 is a potent inhibitor of cathepsin B in vitro but a poor inhibitor of intracellular cathepsin B.

The impact of nitroxoline on tumor cell invasion was also tested on the transformed human breast epithelial cell line, MCF-10A neoT. Using an MTS assay, nitroxoline was shown to be nontoxic on MCF-10A neoT cells up to a concentration of 10 μM (Figure 4a). In a two-dimensional in vitro invasion assay, 10 μM nitroxoline significantly inhibited invasion of MCF-10A neoT cells (40.7% compared with DMSO control; Figure 4b), a process that is enhanced by degradation of the extracellular matrix by cathepsin B.

Cathepsin B was previously shown to contribute significantly to invasion of tumor-cell-derived spheroids implanted in collagen I and Matrigel matrix.[18,19] Tumor spheroids present a three-dimensional in vitro model of tumor invasion, which resembles the in vivo tumor environment more closely than the two-dimensional models because they mimic initial avascular stages of solid tumors in vivo.[20] Therefore nitroxoline was tested in a spheroid model based on implantation of individual cellular aggregates into the Matrigel that served as a surrogate for a basement membrane. In the DMSO control experiment, cells at the border of the aggregate invaded the Matrigel, forming a corona around the original aggregate. Addition of

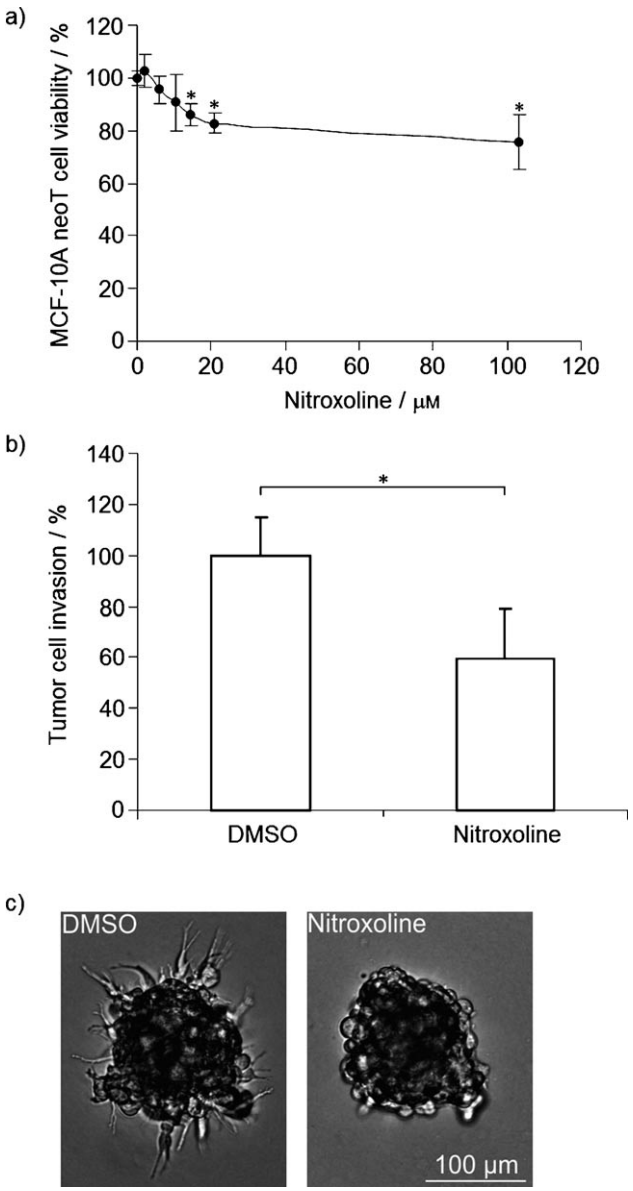

Figure 4. Nitroxoline inhibits tumor cell invasion in vitro. a) Effect of nitroxoline on MCF-10A neoT cell viability was evaluated using an MTS assay. Data are presented as the percentage of viable cells in the presence of increasing nitroxoline concentrations compared to the DMSO control (mean ± SD, $n = 4$). b) Effect of 10 μM nitroxoline on tumor cell invasion as assessed with a two-dimensional in vitro invasion assay. Data are presented as the percentage of invading cells in the presence of DMSO and 10 μM nitroxoline, respectively (mean ± SD, $n = 3$). c) Effect of 10 μM nitroxoline on tumor cell invasion as evaluated with a three-dimensional in vitro tumor model based on cell aggregates implanted in Matrigel.

10 μM nitroxoline completely abrogated the invasive activity at the edge of the aggregate (Figure 4c). The ability of nitroxoline to impair malignant processes was reported in a very recent study.[21] In mice bearing human bladder tumors nitroxoline significantly reduced tumor growth by inhibiting type 2 methionine aminopeptidase and sirtuin 1, the enzymes involved in tumor angiogenesis. It can be expected that simultaneous action of nitroxoline on different tumor targets may contribute synergistically to tumor regression.

To summarize, our results show that nitroxoline is noncovalent, reversible inhibitor of cathepsin B with K_i values comparable to other known reversible inhibitors.[11,12] Its applicability was demonstrated in cell-based assays, where nitroxoline significantly inhibited extracellular and intracellular degradation of ECM, impairing tumor cell invasion. These results and the fact that nitroxoline is an established antimicrobial agent with well-known pharmacokinetics and toxicity profile suggests it has potential as a drug candidate for treating cancer and other diseases associated with increased cathepsin B activity. In addition, the new mechanism of protease inhibition proposed in this study may lead to further structure-based medicinal chemistry approaches to developing novel noncovalent cathepsin B inhibitors as therapeutic agents.

Experimental Section

Compounds **1**–**8** were either purchased or synthesized as previously described.[22] For each compound, the following were determined/performed: melting point, ^{1}H NMR, ^{13}C NMR, IR, MS, HRMS, elemental analyses, and analytical thin layer chromatography. Inhibition constants for compounds **1**–**8** against different cathepsins were determined with enzyme kinetics. Reversibility of nitroxoline inhibition was determined using a rapid dilution test, active site probe DCG-04 and mass spectrometry. To assess the ability of nitroxoline (**1**) to inhibit pathological processes associated with increased cathepsin B endopeptidase activity, various DQ–collagen type IV assays, as well as two- and three-dimensional in vitro invasion assays, were used. For further details, see the Supporting Information.

Acknowledgements

The authors thank Dr. Bogdan Kralj and Dr. Dušan Žigon (Mass Spectrometry Center, Jožef Stefan Institute, Ljubljana, Slovenia) for mass spectral measurements, Dr. Andreja Kovač (Faculty of Pharmacy, University of Ljubljana, Ljubljana, Slovenia) for technical assistance, Dr. Matthew Bogyo (Stanford Medical School, Stanford, USA) for providing DCG-04 probe, Prof. Bonnie Sloane (Wayne State University School of Medicine, Detroit, USA) for providing MCF-10A neoT cells, and Prof. Roger Pain (Department of Biotechnology, Jožef Stefan Institute, Ljubljana, Slovenia) for critical reading of the manuscript. The authors thank SimBioSys Inc. (Toronto, Canada) for free academic license for eHiTS. This work was supported by the Slovenian Research Agency (grant number P4–0127 to J.K.), and partially supported by the European Union 7th Framework Project: Nanophoto (to J.K.).

Keywords: antitumor agents · cancer · cathepsin B · enzyme inhibitors · nitroxolines

[1] J. Kos, T. T. Lah, *Oncol. Rep.* **1998**, *5*, 1349 – 1361.
[2] M. M. Mohamed, B. F. Sloane, *Nat. Rev. Cancer* **2006**, *6*, 764 – 775.
[3] N. D. Rawlings, F. R. Morton, C. Y. Kok, J. Kong, A. J. Barrett, *Nucleic Acids Res.* **2008**, *36*, D320 – D325.
[4] C. Illy, O. Quraishi, J. Wang, E. Purisima, T. Vernet, J. S. Mort, *J. Biol. Chem.* **1997**, *272*, 1197 – 1202.
[5] D. Musil, D. Zucic, D. Turk, R. A. Engh, I. Mayr, R. Huber, T. Popovic, V. Turk, T. Towatari, N. Katunuma, *EMBO J.* **1991**, *10*, 2321 – 2330.
[6] D. K. Nägler, A. C. Storer, F. C. V. Portaro, E. Carmona, L. Juliano, R. Ménard, *Biochemistry* **1997**, *36*, 12608 – 12615.
[7] R. Frlan, S. Gobec, *Curr. Med. Chem.* **2006**, *13*, 2309 – 2327.
[8] B. Turk, *Nat. Rev. Drug Discovery* **2006**, *5*, 785 – 799.
[9] B. Murugasu-Oei, T. Dick, *Int. J. Antimicrob. Agents* **2001**, *18*, 579 – 582.
[10] P. C Almeida, I. L. Nantes, J. R. Chagas, C. C. Rizzi, A. Faljoni-Alario, E. Carmona, L. Juliano, H. B. Nader, I. L. Tersariol, *J. Biol. Chem.* **2001**, *276*, 944 – 951.
[11] G. Z. Zeng, X. L. Pan, N. H. Tan, J. Xiong, Y. M. Zhang, *Eur. J. Med. Chem.* **2006**, *41*, 1247 – 1252.
[12] P. Schenker, P. Alfarano, P. Kolb, A. Caflisch, A. Baici, *Protein Sci.* **2008**, *17*, 2145 – 2155.
[13] B. Y. Feng, B. K. Shoichet, *Nat. Protoc.* **2006**, *1*, 550 – 553.
[14] D. Turk, M. Podobnik, T. Popovic, N. Katunuma, W. Bode, R. Huber, V. Turk, *Biochemistry* **1995**, *34*, 4791 – 4797.
[15] I. Stern, N. Schaschke, L. Moroder, D. Turk, *Biochem. J.* **2004**, *381 (Pt. 2)*, 511 – 517.
[16] J. Praznikar, P. V. Afonine, G. Guncar, P. D. Adams, D. Turk, *Acta Crystallogr. Sect. D* **2009**, *65*, 921 – 931.
[17] K. Tomoo, *Curr. Top. Med. Chem.* **2010**, *10*, 696 – 707.
[18] L. Sevenich, U. Schurigt, K. Sachse, M. Gajda, F. Werner, S. Müller, O. Vasiljeva, A. Schwinde, N. Klemm, J. Deussing, C. Peters, T. Reinheckel, *Proc. Natl. Acad. Sci. USA* **2010**, *107*, 2497 – 2502.
[19] K. K. Veeravalli, C. Chetty, S. Ponnala, C. S. Gondi, S. S. Lakka, D. Fassett, J. D. Klopfenstein, D. H. Dinh, M. Gujrati, J. S. Rao, *PLoS One* **2010**, *5*, e11583.
[20] J. M. Kelm, N. E. Timmins, C. J. Brown, M. Fussenegger, L. K. Nielsen, *Biotechnol. Bioeng.* **2003**, *83*, 173 – 180.
[21] J. S. Shim, Y. Matsui, S. Bhat, B. A. Nacev, J. Xu, H. E. Bhang, S. Dhara, K. C. Han, C. R. Chong, M. G. Pomper, A. So, J. O. Liu, *J. Natl. Cancer Inst.* **2010**, *102*, 1855 – 1873.
[22] M. Movrin, D. Maysinger, E. Marok, *Pharmazie* **1980**, *35*, 458 – 460.

Received: February 17, 2011
Revised: April 4, 2011
Published online on May 20, 2011

